

Electrically Coupling Multifunctional Oxides to Semiconductors: A Route to Novel Material Functionalities

J. H. Ngai¹, K. Ahmadi-Majlan¹, J. Moghadam¹, M. Chrysler¹, D. P. Kumah², C. H. Ahn², F. J. Walker², T. Droubay³, M. Bowden⁴, S. A. Chambers³, X. Shen⁵, D. Su⁵

¹Department of Physics, University of Texas-Arlington, Arlington, TX 76019, U.S.A.

²Department of Applied Physics and Center for Research on Interface Structures and Phenomena, Yale University, New Haven, CT 06511, U.S.A.

³Physical Sciences Division, Pacific Northwest National Laboratory, Richland, WA 99352, U.S.A.

⁴Environmental Molecular Sciences Laboratory, Pacific Northwest National Laboratory, Richland, WA 99352 , U.S.A.

⁵Center for Functional Nanomaterials, Brookhaven National Laboratory, Upton, NY 11973, U.S.A.

ABSTRACT

Complex oxides and semiconductors exhibit distinct yet complementary properties owing to their respective ionic and covalent natures. By electrically coupling oxides to semiconductors within epitaxial heterostructures, enhanced or novel functionalities beyond those of the constituent materials can potentially be realized. Key to electrically coupling oxides to semiconductors is controlling the physical and electronic structure of semiconductor – crystalline oxide heterostructures. Here we discuss how composition of the oxide can be manipulated to control physical and electronic structure in $\text{Ba}_{1-x}\text{Sr}_x\text{TiO}_3/\text{Ge}$ and $\text{SrZr}_x\text{Ti}_{1-x}\text{O}_3/\text{Ge}$ heterostructures. In the case of the former we discuss how strain can be engineered through composition to enable the re-orientable ferroelectric polarization to be coupled to carriers in the semiconductor. In the case of the latter we discuss how composition can be exploited to control the band offset at the semiconductor - oxide interface. The ability to control the band offset, i.e. band-gap engineering, provides a pathway to electrically couple crystalline oxides to semiconductors to realize a host of functionalities.

INTRODUCTION

Developing materials that exhibit enhanced or novel functionalities is essential to address present challenges in energy harvesting and information technology. Heterostructures comprised of materials that exhibit dissimilar yet complementary electrical properties present a new approach to realize novel material functionalities. Key to realizing novel and enhanced functionalities in such composite structures is coupling the electrical properties of the constituent materials.

In this regard, heterostructures comprised of covalently bonded semiconductors and ionic crystalline complex oxides are of particular interest due to the complementary properties exhibited by these materials. Complex oxides exhibit properties such as ferromagnetism, ferroelectricity and strongly correlated phenomena such as metal-insulator transitions. In comparison, semiconductors exhibit high carrier mobilities at room temperature and direct band-gaps. Thus, monolithically integrating crystalline oxides with semiconductors enables their respective properties to be potentially coupled to realize functionalities beyond either constituent material [1] [2] [3].

Perovskite structured complex oxides (ABO_3) are of particular interest since they are largely lattice-matched to (100) surfaces of diamond cubic structured semiconductors, such as Si, Ge and GaAs. Furthermore, a broad range of material behaviors can be realized by tuning the stoichiometry of the *A*- and *B*-site cations. The pioneering work of McKee *et al.* enabled single crystalline $SrTiO_3$ to be grown on semiconductors with atomically abrupt and structurally coherent interfaces using oxide molecular beam epitaxy (MBE) [4]. The epitaxial growth of $SrTiO_3$ on semiconductors provides an epitaxial platform by which multifunctional oxides can be monolithically integrated on semiconductors.

Beyond monolithic integration, control of both physical and electronic structure of semiconductor – crystalline oxide heterostructures is essential to control electrical coupling between the two materials. Here we discuss how composition of the *A*- and *B*-site cations within the perovskite structure can be exploited to engineer strain (physical structure) and band alignment (electronic structure) in semiconductor-oxide heterostructures. Specifically, we discuss how *A*- site composition of $Ba_{1-x}Sr_xTiO_3$ (BST) can be tuned layer-by-layer to control compressive strain in BST/Ge heterojunctions. Compressive strain enables the re-orientable ferroelectric polarization of BST to be coupled to carriers in Ge [5]. In regards to band alignment, we will show how control of *B*-site composition of $SrZr_xTi_{1-x}O_3$ (SZTO) can be exploited to tune the band alignment between of SZTO and Ge [6]. Analogous to band gap engineering at heterojunctions between III-V semiconducting materials, the control of band alignment at the SZTO/Ge heterojunction provides a platform to electrically couple multifunctional oxides to semiconductors.

EXPERIMENT

$BaTiO_3/Ba_{1-x}Sr_xTiO_3$ on Ge: Engineering strain in semiconductor-crystalline oxide heterostructures

Electrically coupling the re-orientable polarization of a ferroelectric to a semiconductor remains a long standing challenge in materials research. Such semiconductor – ferroelectric heterojunctions have long been of interest for a variety of applications, including memory, non-volatile and ultra-low power logic, and sensing technologies [7] [8] [9] [10]. Single crystalline ferroelectrics on semiconductors are ideal for such applications, since they offer superior material characteristics in comparison to polycrystalline materials.

Despite the ability to epitaxially grow single crystalline ferroelectrics on semiconductors, electrically coupling the polarization of the former to the latter remains challenging. One challenge is maintaining c-axis oriented growth associated with an out-of-plane polarization for thicker ferroelectric films. Thicker films are generally required to offset depolarization fields and maintain ferroelectric behavior when grown on a semiconducting electrode [11]. However,

epitaxial films of BaTiO_3 (BTO) grown on Ge relax for thicknesses exceeding 10 nm due to the difference in lattice constants at elevated growth temperatures. As relaxed films are cooled through the Curie temperature, tensile strain is imparted to the BTO from the Ge substrate, since the former has a much larger coefficient of thermal expansion than the latter. Consequently, BTO grown on Ge is a-axis orientated, associated with a ferroelectric polarization that lies predominantly in the plane of the film. For example, Fig. 1 (red dotted) shows x-ray diffraction data for a 40 nm thick BTO film grown on Ge indicating a-axis oriented growth [5].

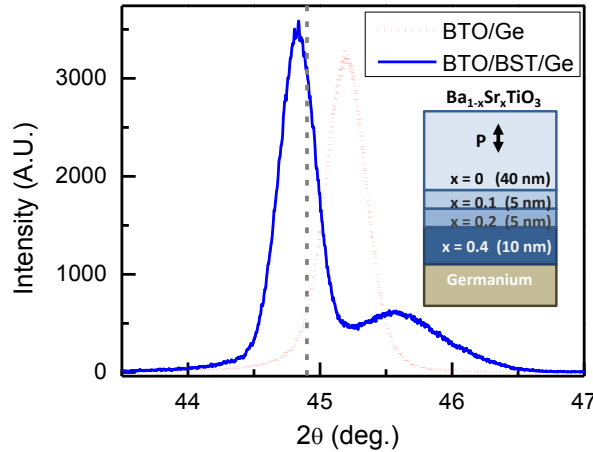


Figure 1. X-ray diffraction data of a 40 nm thick BTO film grown on Ge (red dotted) and a Sr-alloyed BST heterostructure (blue solid) illustrated in the inset. The BST heterostructure exhibits c-axis oriented growth, as indicated by the grey dashed vertical line of the c-axis lattice constant of bulk BTO. Figure reproduced with permission from Ref. [5].

Compressive strain can be utilized to offset the effects of thermal expansion mismatch and achieve an out-of-plane polarization of BTO grown on Ge. The effects of compressive strain on ferroelectrics, such as BTO, have been extensively investigated [12]. Whereas such prior studies achieved compressive strain through growth on oxide substrates that have smaller in-plane lattice constants, a different approach to impart compressive strain will be required since the semiconductor cannot be arbitrarily changed in our BTO-Ge heterojunctions. Compressive strain can be achieved by inserting an epitaxial buffer layer that has a smaller in-plane lattice constant than BTO. For example, a single layer of $\text{Ba}_{0.7}\text{Sr}_{0.3}\text{TiO}_3$ was inserted as a buffer to achieve c-axis oriented growth of BTO on Si [13]. Similarly, SrTiO_3 has been used as a buffer to achieve c-axis oriented growth of BTO on GaAs and Ge [14] [15]. Here, we do a variation of the single-layer buffer approach by growing a graded structure comprised of 4 layers, with increasing Sr content x for the layers approaching the Ge substrate. This graded structure allows for very thick c-axis oriented BTO films to be grown, and enables the compressive strain to be tuned via the Sr distribution within the graded buffer [16]. Figure 1 shows x-ray diffraction for a Sr-alloyed heterostructure (blue), in which two peaks are observed. The smaller peak on the right is associated with the Sr alloyed layers whereas the larger peak on the left is associated with the thicker BTO layer. The c-axis orientation of the BTO film is indicated by the grey dashed line, which shows where bulk c-axis lattice constant is expected to lie.

The c-axis oriented growth enables the polarization of BTO to be coupled to Ge, as manifested through current-voltage characteristics shown in Fig. 2. The conduction bands of

BTO/BST are nearly aligned with the conduction bands of Ge. The near alignment of conduction bands at interfaces between BTO/BST and Ge facilitates charge transport and suggests that rectifying behavior should be exhibited by such heterojunctions, provided a counter electrode forming an interface with finite barrier for charge transport can be created on the BTO surface. To explore the possibility of diode-like transport, Pt electrodes are deposited on the BTO surface, and electrical transport measurements are performed in the geometry illustrated in the inset of Fig. 2. Representative current-voltage characteristics of a Pt/BTO/BST/Ge heterostructure are shown in Fig. 2. For c-axis oriented heterostructures, rectifying behavior and hysteresis are observed (blue solid). The rectifying transport arises from the asymmetry of the metal/ferroelectric/semiconductor heterojunction, namely, the presence (absence) of a potential barrier at the Pt/BTO (BST/Ge) interface for carrier transport. The hysteretic behavior arises from switching of the ferroelectric polarization in the c-axis oriented heterostructure, which modulates the Schottky barrier height at the BTO-Ge interface [17] [18]. The association between the hysteresis and switching of the ferroelectric polarization is confirmed by current-voltage characteristics of an a-axis oriented Pt/BTO/Ge heterostructure, which is shown (red dashed) in Fig. 2. The transport characteristics of the a-axis oriented film exhibit rectifying behavior but negligible hysteresis, since the polarization lies in the plane of the film and cannot couple to electric fields applied in the out-of-plane direction.

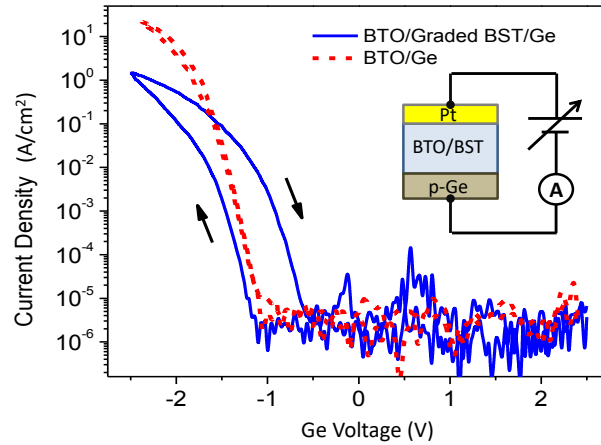


Figure 2. Current-Voltage characteristics of a BTO/BST/Ge heterostructure (blue) and a BTO/Ge heterostructure (red dashed). The former (latter) has c-axis (a-axis) orientation and exhibits (does not exhibit) hysteresis. Figure reproduced with permission from Ref. [5].

The presence (absence) of hysteresis in c-axis (a-axis) oriented BTO-Ge heterostructures demonstrates that physical structure has a profound effect on electrical coupling between multifunctional oxides and semiconductors. Here we have demonstrated that compositional grading of the perovskite A-site can be exploited to control strain in semiconductor –crystalline oxide heterojunctions. Beyond physical structure, control of electronic structure, namely, the band alignment at interfaces is also essential to electrically couple multifunctional oxides to semiconductors. Below we discuss how composition can also be exploited to control band offset at semiconductor – crystalline oxide heterojunctions.

SrZ_xTi_{1-x}O₃ on Ge: Bandgap engineering at semiconductor-crystalline oxide interfaces

For many applications envisioned for semiconductor – ferroelectric heterojunctions, the ferroelectric is required to behave as a capacitor in which polarization is coupled to the semiconductor, but charge transport is inhibited. Thus the BST-Ge heterojunctions discussed in the preceding section are not ideal for such applications. The charge transport through the BST-Ge heterojunction arises from the type-II band alignment at the interface, in which the conduction band of the oxide is below the conduction band of the semiconductor. To prevent charge transport, an intermediary oxide layer that has a type-I offset is necessary, in which the conduction band of the oxide is above the conduction band of the semiconductor. Beyond ferroelectrics, a type-I offset at a semiconductor-crystalline oxide interface also enables dielectric and ferromagnetic properties of multifunctional oxides to be coupled to semiconductors.

Here we show that compositional control within semiconductor – crystalline oxide heterostructures can also be exploited to manipulate band alignment at semiconductor – crystalline oxide interfaces. Our model system is SZTO grown on Ge using oxide MBE, in which the band gap and offset are controlled through Zr content x . By controlling the Zr content, the bandgap of SZTO can be tuned from 3.2 eV to 5.6 eV, which are the bandgaps of the two end members of the solid-solution, namely, SrTiO₃ and SrZrO₃ respectively.

Careful control of growth conditions enables single-crystalline SZTO to be grown on Ge, with atomically abrupt and structurally coherent interfaces. Reflection high energy electron diffraction (RHEED) in combination with x-ray diffraction survey scans of SZTO films of various Zr content grown on Ge confirm single crystalline growth [6]. In general, the sharpness of the RHEED streaks improved and the XRD rocking curve widths decreased with Zr content, which we attribute to improved lattice matching between the SZTO and Ge. Scanning transmission electron microscopy (STEM) measurements provide atomic scale images of the film and interfacial structure between SZTO and Ge. Figure 3 is a high-angle annular dark field (HAADF) image of a $x = 0.70$ film, showing an abrupt heterojunction, with no extended interfacial phases comprised of amorphous GeO_x. The alternating *A* - and *B* -site planes that comprise the perovskite structure of SZTO are particularly clear due to the closely matched atomic masses of Sr and Zr.



Figure 3. High angle annular dark field image of the SZTO-Ge interface for Zr content $x = 0.7$.

Current-voltage characterization of leakage current through SZTO-Ge heterojunctions demonstrate that the band offset can be tuned from type-II to type-I through Zr content. Figure 4 shows current-voltage measurements through the SZTO-Ge heterojunctions, where the bias is applied to a Ni electrode deposited on top of the SZTO. To elucidate the effect of Zr substitution in creating a band offset, measurements of an equivalently thick 38 u.c. (≈ 15 nm) BST ($\text{Ba}_{0.4}\text{Sr}_{0.6}\text{TiO}_3$) film is also shown. For higher Zr content x , the SZTO-Ge heterojunctions exhibit leakage current that is orders of magnitude less than the BST-Ge heterojunction, consistent with the presence of a type-I band offset [6]. It should be noted that the flat regions observed between 0 and -1 V for $x = 0.45$ and 0.75 are due in part to the resolution limit in our instrumentation. Also, an asymmetry in the current-voltage characteristics is observed about zero-bias for SZTO-Ge and BST-Ge heterojunctions, which we attribute to a difference in barrier heights for gate and substrate injection.

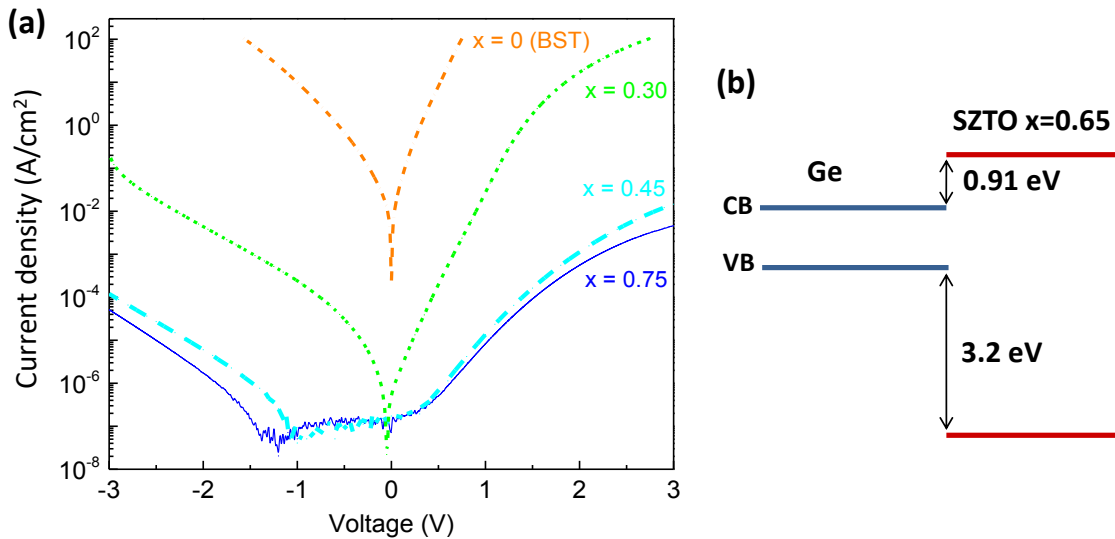


Figure 4. (a) Current-voltage characteristics of a 38 u.c. thick SZTO-Ge heterojunction and a 38 u.c. thick BST-Ge heterojunction. SZTO-Ge heterojunctions exhibit significantly less leakage than BST-Ge heterojunctions, consistent with the presence of a type-I conduction band offset. (b) X-ray photoemission spectroscopy measurements quantify the offsets as shown for a $x = 0.65$ film. Figures reproduced with permission from Ref. [6].

To quantify the band offsets of SZTO on Ge, high-resolution core-level (CL) and valence band (VB) x-ray photoemission measurements on a $x = 0.65$ film have been performed. We used a combination of CL and VB spectra for thin and thick film samples to determine the valence band offset (VBO). The energy from the top of the VB to the $\text{Sr}^{3d\ 5/2}$ core peak, ($E_{\text{Sr}^{3d\ 5/2}} - E_{\text{V}}$)_{SZTO}, was measured to be 130.59(6) eV for a 38 u.c. film. This quantity was combined with an energy difference for clean Ge(110) [19], ($E_{\text{Ge}^{3d\ 5/2}} - E_{\text{V}}$)_{Ge} = 29.52(4) eV, and the core-level binding energy difference for a 6 u.c. heterojunction, ($E_{\text{Sr}^{3d\ 5/2}} - E_{\text{Ge}^{3d\ 5/2}}$)_{HJ} = 104.27(2) eV, to yield a VBO given by $\Delta E_{\text{V}} = (E_{\text{Sr}^{3d\ 5/2}} - E_{\text{Ge}^{3d\ 5/2}})_{\text{HJ}} + (E_{\text{Ge}^{3d\ 5/2}} - E_{\text{V}})_{\text{Ge}} - (E_{\text{Sr}^{3d\ 5/2}} - E_{\text{V}})_{\text{SZTO}} = 3.20(8)$ eV, as illustrated in Fig. 4(b). On the premise the bandgap of SZTO follows Vegard's law, the conduction band offset for $x = 0.65$ is estimated to be 0.91 eV, confirming the presence of a type-I offset.

DISCUSSION

SZTO provides both an epitaxial platform and electrical platform for integrating and electrically coupling multifunctional oxides to semiconductors. Previously, SrTiO_3 has been utilized as an epitaxial platform in which it acts as an epitaxial buffer between the semiconductor and multifunctional oxides. However, the fixed type-II band alignment of SrTiO_3 limits control of electrical coupling between the multifunctional oxide and semiconductor [20] [21]. In comparison, the tunable band offset of SZTO enables a variety of multifunctional oxides to be coupled to semiconductors. For example, SZTO could serve as an intermediate layer to inhibit charge transfer from a ferroelectric to a semiconductor, thus enabling a capacitor to form. As an intermediate buffer, the relatively high- κ would reduce effects of depolarization fields in the ferroelectric. For spintronic applications, SZTO could serve as a tunnel barrier through which spin-polarized carriers from a crystalline half-metallic oxide can be injected into a semiconductor. Injection via tunneling mitigates the large conductivity mismatch between the metallic ferromagnetic oxide and semiconductor, thereby enabling more efficient injection [22]. Furthermore, the barrier height of SZTO is adjustable through control of Zr content, which could greatly enhance injection efficiencies. Future work will exploit the tunable band offset of SZTO to realize a host of functionalities in semiconductor – crystalline oxide heterostructures.

CONCLUSIONS

Semiconductor – crystalline oxide heterostructures provide a setting in which complementary properties can be coupled to realize novel functionalities beyond either constituent material. Elucidating how crystalline oxides can be electrically coupled to semiconductors is essential to realize novel functionalities in such heterostructures. Control of physical structure and electronic structure of semiconductor – crystalline oxide heterostructures is essential to achieving electrical coupling. We have demonstrated that control of the composition of both *A*- and *B*-sites within the perovskite structure can be exploited to engineer strain in semiconductor – crystalline oxide heterostructures and band alignment at interfaces. Control of both strain and band alignment enables novel functionalities to emerge in semiconductor – oxide heterostructures.

ACKNOWLEDGMENTS

This work was supported by the University of Texas at Arlington and the National Science Foundation (NSF) under DMR-1508530. The work performed at Yale University was supported by the NSF under MRSEC DMR-1119826 and DMR-1309868. The work performed at Brookhaven National Laboratory was supported by U.S. Department of Energy, Office of Basic Energy Sciences, under Contract No. DEAC02- 98CH10886. The work performed at Pacific Northwest National Laboratory was supported by the U.S. Department of Energy, Office of Science, Division of Materials Sciences and Engineering under Award 10122.

REFERENCES

- [1] J. W. Reiner, A. M. Kolpak, Y. Segal, K. F. Garrity, S. Ismail-Beigi, C. H. Ahn and F. J. Walker, *Adv. Mater.* , vol. 22, p. 2919, 2010.
- [2] A. A. Demkov and A. B. Posadas, *Integration of Functional Oxides with Semiconductors*, New York: Springer-Verlag, 2014.
- [3] S. H. Baek and C. -B. Eom, *Acta Materiala*, vol. 61, p. 2734, 2013.
- [4] R. A. McKee, F. J. Walker and M. F. Chisholm, "," *Phys. Rev. Lett.*, vol. 81, pp. 3014-3017, 1998.
- [5] J. H. Ngai, D. P. Kumah, C. H. Ahn and F. J. Walker, "," *Appl. Phys. Lett.*, vol. 104, p. 062905, 2014.
- [6] J. Moghadam, K. Ahmadi-Majlan, X. Shen, T. Droubay, M. Bowden, M. Chrysler, D. Su, S. A. Chambers and J. H. Ngai, *Adv. Mater. Interfaces* , vol. 2, p. 1400497, 2015.
- [7] K. Takahashi, K. Aizawa, B. -E. Park and H. Ishiwara, *Jap. J. Appl. Phys.*, vol. 44, pp. 6218-6220, 2005.
- [8] S. Salahuddin and S. Datta, *Nano Lett.*, vol. 8, pp. 405-410, 2008.
- [9] O. Auciello, C. A. P. de Araujo and J. Selinska, "Review of the Science and TECnology for Low- and High-Density Nonvolatile Ferroelectric Memories," in *Emerging Non-volatile Memories*, New York, Springer, 2014.
- [10] N. Setter, D. Damjanovic, L. Eng, G. Fox, S. Gevorgian, S. Hong, A. Kingon, H. Kohlstedt, N. Y. Park, G. B. Stephenson, I. Stolitchnov, A. K. Tagantsev, D. V. Taylor, T. Yamada and S. Streiffer, *J. Appl. Phys.*, vol. 100, p. 051606, 2006.
- [11] J. W. Reiner, F. J. Walker, R. A. McKee, C. A. Billman, J. Junquera, K. M. Rabe and C. H. Ahn, *Phys. Stat. Solidi B*, vol. 241, pp. 2287 - 2290, 2004.
- [12] K. J. Choi, M. Biegalski, Y. L. Li, A. Sharan, J. Schubert, R. Uecker, P. Reiche, Y. B. Chen, X. Q. Pan, V. Gopalan, L. -Q. Chen, D. G. Schlom and C. B. Eom, *Science*, vol. 306, p. 1005, 2004.
- [13] V. Vaithyanathan, J. Lettieri, W. Tian, A. Sharan, A. Vasudevarao, Y. L. Li, A. Kochhar, H. Ma, J. Levy, P. Zschack, J. C. Woicik, L. Q. Chen, V. Gopalan and D. G. Schlom, "c-axis oriented epitaxial BaTiO₃ films on (001) Si," *J. Appl. Phys.*, vol. 100, p. 024108, 2006.
- [14] R. Contreras-Guerrero, J. P. Veazey, J. Levy and R. Droopad, *Appl. Phys. Lett.*, vol. 102, p. 012907, 2013.
- [15] P. Ponath, K. Fredrickson, A. B. Posadas, Y. Ren, X. Wu, R. K. Vasudevan, M. B. Okatan, S. Jesse, T. Aoki, M. R. McCartney, D. J. Smith, S. V. Kalinin, K. Lai and A. A. Demkov, *Nat. Comm.*, vol. 6, p. 6067, 2014.
- [16] J. H. Ngai et al., *in preparation*, 2016.
- [17] A. Klein and F. Chen, *Phys. Rev. B*, vol. 86, p. 094105, 2012.
- [18] Z. Wen, C. Li, D. Wu, A. Li and N. Ming, *Nat. Mater.*, vol. 12, p. 617, 2013.
- [19] The difference in energy between the valence band to Ge3d for Ge(110) was taken from the literature. The value for Ge(100) will differ from Ge(110) by only a few hundredths of an eV.
- [20] S. A. Chambers, Y. Liang, Z. Yu, R. Droopad and J. Ramdani, *J. Vac. Sci. Technol. A*, vol. 19, pp. 934 - 937, 2001.
- [21] F. Amy, A. Wan, A. Kahn, F. J. Walker and R. A. McKee, *J. Appl. Phys.*, vol. 96, pp. 1601-

1606, 2004.

[22] I. Zutic, J. Fabian and S. Das Sarma, *Rev. Mod. Phys.*, vol. 76, p. 323, 2004.